

# Advanced Information Feedback Coupled with an Evolutionary Game in Intelligent Transportation Systems

Chuanfei Dong, Yuxi Chen, Xu Ma and Bokui Chen

**Abstract** It has been explored for decades how to alleviate traffic congestions and improve traffic fluxes by optimizing routing strategies in intelligent transportation systems (ITSs). It, however, has still remained as an unresolved issue and an active research topic due to the complexity of real traffic systems. In this study, we propose two concise and efficient feedback strategies, namely mean velocity difference feedback strategy and congestion coefficient difference feedback strategy. Both newly proposed strategies are based upon the time-varying trend in feedback information, which can achieve higher route flux with better stability compared to previous strategies proposed in the literature. In addition to improving feedback strategies, we also investigate information feedback coupled with an evolutionary game in a 1-2-1-lane ITS with dynamic periodic boundary conditions to better mimic the driver behavior at the 2-to-1 lane junction, where the evolutionary snowdrift game is adopted. We propose an improved self-questioning Fermi (SQF) updating mechanism by taking into account the self-play payoff, which shows several advantages compared to the classical Fermi mechanism. Interestingly, our model calculations show that the SQF mechanism can prevent the system from being enmeshed in a globally defective trap, in good agreement with the analytic solutions derived from the mean-field approximation.

---

C. Dong (✉) · Y. Chen  
AOSS Department, College of Engineering, University of Michigan,  
Ann Arbor, MI 48109, USA  
e-mail: dcfy@umich.edu

X. Ma  
Department of Physics, Syracuse University, Syracuse, NY 13244, USA

B. Chen  
Department of Electronic and Information Engineering, Hong Kong Polytechnic University,  
Hung Hom, Kowloon, Hong Kong

B. Chen  
Division of Logistics and Transportation, Graduate School at Shenzhen,  
Tsinghua University, Shenzhen 518055, People's Republic of China

**Keywords** Advanced information feedback · Two-route guidance strategy · Cellular automaton model · Evolutionary game theory · Snowdrift game · Stochastic Fermi rule · Self-questioning updating rule · Self-play payoff · Intelligent transportation system · Mean-field approximation

## 1 Introduction

Cooperation is ubiquitous in economic and social systems [13]. These systems are filled with selfish individuals who try to maximize their own benefits. But being contrary to the view of the Darwinian selection, cooperation becomes the main behavior of these systems. The emergence of cooperation in selfish circumstances has therefore attracted much attention from physicists recently. Game theory, together with its extensions, provides a useful framework to investigate this problem [2, 31, 51]. In the recent years game theory has been introduced into traffic flow studies and related fields to solve conflicts when two or more vehicles or pedestrians compete for an empty space [7, 24, 26, 37, 40, 43, 46, 50, 55, 56, 58, 60]. For instance, Perc [43] introduced the evolutionary game between neighboring agents in the Biham-Middleton-Levine (BML) model, and he found that a traffic flow seizure is induced. The evolutionary game was also introduced into random walk to study immigration behaviors [46] and into unidirectional pedestrian flow to study its phase transition behaviors [26]. Tanimoto et al. [50] and Zheng and Cheng [60] introduced game theory to study the evacuation process. Furthermore, Wang et al. [55] proposed a memory-based Snowdrift Game (SG) [45] on networks which abandon the learning mechanism. Instead, a self-questioning mechanism and a memory-based updating rule were adopted. Gao et al. [24] extended this work and studied both the evolutionary Prisoner's Dilemma Game (PDG) [3] and Snowdrift Game (SG) [45] with a self-questioning mechanism combined with a stochastic evolutionary rule, mainly on a scale-free traffic network. In Gao et al. [24], they found the so-called "Cooperative Ping-pong Effect" occurs in both games in certain cases, and plays an important role in determining the behavior of the whole system. However, none of these studies incorporated the effect of information feedback into an evolutionary game.

For some socioeconomic systems, it is desirable to provide real-time information or a short-term forecast about dynamics. For instance, in stock markets it is advantageous to give a reliable forecast in order to maximize profits. In traffic flow, advanced traveler information systems (ATIS) provide real-time information about traffic conditions to road users by means of communication such as variable message signs, radio broadcasts, or on-board computers [1]. The aim is to help individual road users to minimize their personal travel time. Therefore traffic congestion can be alleviated, and the capacity of the existing infrastructure is used more efficiently. Figure 1 shows a schematic diagram of an information feedback system, which demonstrates that feedback information plays a significant role in the

## An Information Feedback System

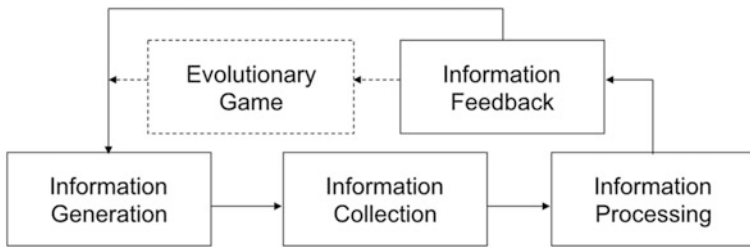


**Fig. 1** The schematic diagram of information feedback coupled with an evolutionary game in an intelligent information system

loop. An intelligent transportation system (ITS) is an example of such information feedback system in our daily life. The vehicle behavior and dynamics based on the advanced information feedback in an ITS is an important research topic due to its high efficiency in controlling spatial distribution of traffic patterns.

Traffic flow and related problems have attracted considerable attention in the past decade [12, 28, 38, 42]. Understanding the characteristics of the city traffic is one of the most essential parts in the community of traffic research. This leads to the fact that traffic flow models have been studied increasingly. In order to understand significant traffic flow phenomena, traffic models such as the kinetic theory [6, 29], fluid-dynamical model [32], car-following model [25, 49] and cellular automaton (CA) model [5, 8, 36, 39, 57] have been investigated. In particular, the first CA traffic model, the Nagel-Schreckenberg model [39] is so far the most popular cellular automaton model in analyzing the traffic flow due to its simplicity and features which can well reproduce real traffic flows. Modeling traffic flow dynamics by cellular automata models has constituted the subject of intensive research by statistical physics during the past few years [12, 28]. However, it still remains an unresolved issue to propose an optimal information feedback strategy in order to essentially improve the road capacity in intelligent transportation systems (ITSs). Recently, dynamics of traffic flow based on a two-route model [52] with advanced information feedbacks have been intensively investigated [9–11, 15–17, 20–22, 27, 30, 33, 35, 44, 52–54, 59]. The route-choice strategy has also been extended to the three-route and crossing traffic systems [14, 18, 19, 23].

Each feedback strategy has its strength and weakness, e.g., Travel Time Feedback Strategy (TTFS) [52] brings a lag effect to make it impossible to provide the road users with the real situation of each route; for Mean Velocity Feedback Strategy (MVFS) [35], the random brake mechanism of the Nagel-Schreckenberg (NS) model [39] brings fragile stability of velocity [54]. In order to provide a concise and efficient feedback, two strategies named Mean Velocity Difference Feedback Strategy (MVDFS) and Congestion Coefficient Difference Feedback Strategy (CCDFS) are proposed. In contrast to Mean Velocity Feedback Strategy (MVFS) and Congestion Coefficient Feedback Strategy (CCFS), the two newly proposed feedback strategies depend on the variation of parameters from time  $t_1$  to

$t_2$ , and  $\Delta t = t_2 - t_1$  is the time difference. Compared with Prediction Feedback Strategy (PFS) [14, 15, 19], the new feedback strategies are implemented with higher efficiency since estimates of the future road conditions in each iteration are not required. It is noteworthy that [20, 22] studied the situation where 75 % drivers exhibit aggressive behavior with the rest 25 % drivers exhibiting timid behavior near the exit, which is similar to the study of [34]. The aggressive and timid behaviors are analogous to the defection and cooperation in an evolutionary game. Dong and Ma [22] found that the aggressive behavior can cause traffic congestions near the exit especially in high-density phases and make the route saturated in a relatively low density state, which is consistent to the results shown by Perc [43].

In this study, we couple the advanced information feedback with the evolutionary SG game and the self-questioning Fermi updating mechanism (including the self-play payoff) to study the evolution of cooperation in a 1-2-1 route intelligent transportation system with dynamic periodic boundary conditions (Fig. 2). The

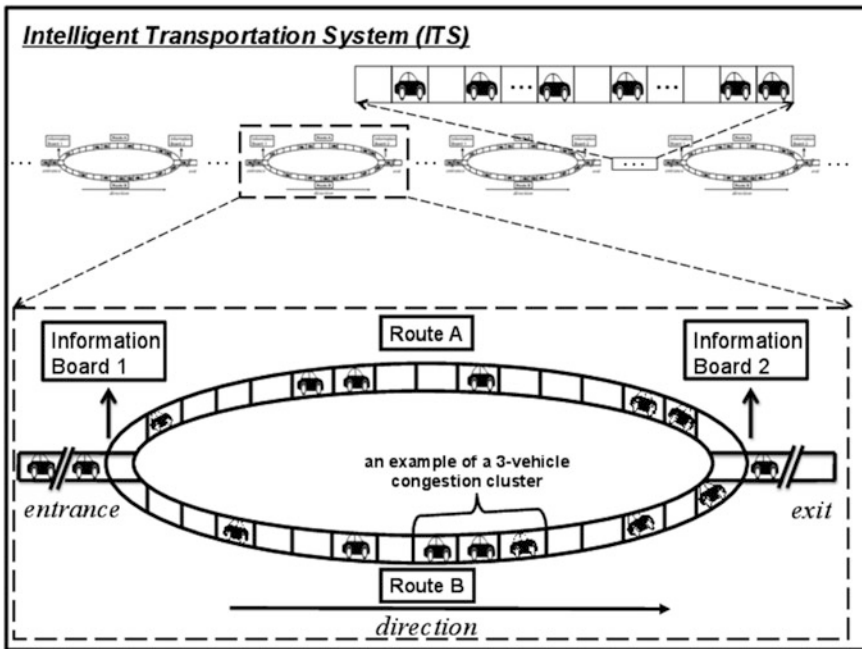


**Fig. 2** The schematic diagram of an intelligent transportation system (ITS). We study one ITS pattern with dynamic periodic boundary conditions in the *dashed box* to represent the whole ITS. The lane between two ITS patterns is assumed to be long enough to hold all the waiting cars that cannot enter the system immediately. There are information boards at both entrance and exit of each ITS pattern. In each ITS pattern, two routes are assumed for simplicity, i.e., route A and route B. The dynamic drivers at the entrance follow the information feedback on board 1 while the static drivers ignore them and enter one route randomly. At the exit, when both players choose to cooperate, the cooperators will leave the ITS pattern based on the information shown on the information board 2. It is noteworthy that when we mention an ITS in the chapter, we refer to this ITS pattern with dynamic periodic boundary conditions

information feedback makes the evolutionary game unique in intelligent transportation systems. As indicated by the dashed box (Fig. 1), when cooperations take place, cooperators leave the exit in according to feedback information instead of randomly. We report the simulation results adopting four different feedback strategies MVFS, CCFS, MVDFS, and CCDFS using a revolutionary coupling approach. The remainder of this chapter is as follows: In Sect. 2, we clarify the notion and briefly introduce the evolutionary game theory, the Nagel-Schreckenberg (NS) model, the two-route model proposed by Wahle et al. [52], the exit scenario, and four feedback strategies: MVFS, CCFS, MVDFS and CCDFS. We present and discuss the simulation results and analyze the results in Sect. 3. Finally, we summarize our conclusions in the last section.

## 2 The Models and Feedback Strategies

### 2.1 Notations

Unless noted otherwise all the notations in this chapter are the same as in Table 1.

### 2.2 Evolutionary Game Theory

At the most elementary level, many evolutionary games can be formalized as two-person games in which each player can either cooperate (C) or defect (D). In sociology and economics, the Prisoner's Dilemma Game (PDG) [3] and Snowdrift Game (SG) [45] have been widely used to model a situation in which mutual cooperation leads to the best outcome in social terms, but defectors can benefit the most individually. In mathematical terms, this is described by a payoff matrix (Table 2, lower panel: entries correspond to the row player's payoffs), where mutual cooperation yields the reward  $R$ , mutual defection leads to punishment  $P$ , and the mixed choice gives the cooperator the sucker's payoff  $S$  and the defector the temptation  $T$ . Game theory has restricted a precondition of  $2R > T + S$ . For mutual cooperation, the society benefits the most, thus corresponding to the largest total payoff. In the PDG, the rank of the four payoff values is  $T > R > P > S$ , while in the SG it is  $T > R > S > P$ , so the SG is more favorable to sustain the cooperative behavior. In a real traffic system, especially a 1-2-1 route ITS, the SG is more appropriate than PDG in order to avoid collisions when both players choose to defect. Therefore, we adopt the SG in this chapter. The number in the payoff matrix shown in Table 3 describes the probability of a vehicle leaving the exit when the driver plays the game with its neighbor on an alternative route. In order to satisfy the payoff rank of the SG, we adopt small quantities  $\epsilon$  and  $\delta$  in the payoff matrix. As will be shown later,  $\epsilon$  and  $\delta$  represent the advanced characteristics that are unique to the intelligent transportation systems whereas the numbers themselves do not represent these effects. Here we set

**Table 1** Major notations

$F_i$	The flux of route $i$
$L_i$	The length of route $i$
$N_i$	The number of vehicles on route $i$
$\rho_i$	The vehicle density on route $i$ , $\rho_i = N_i/L_i$
$N_{tot}$	The total number of vehicles in the traffic system
$N_c$	The number of cooperators in the traffic system
$N_d$	The number of defectors in the traffic system
$V_{mean}^i$	The mean velocity of all the vehicles on route $i$
$v_i$	The velocity of the $i$ th vehicle
$v_{max}$	The maximum velocity of vehicles
$x_i$	The position of the $i$ th vehicle
$g_i$	The number of empty cells in front of vehicle $i$
$n_j$	The number of vehicles of the $j$ th congestion cluster
$q$	The number of congestion clusters on one route
$C$	The congestion coefficient
$V_D$	The mean velocity difference
$C_D$	The congestion coefficient difference
$\Delta t_c$	The time difference in the congestion coefficient difference feedback strategy (CCDFS)
$\Delta t_v$	The time difference in the mean velocity difference feedback strategy (MVDFS)
$P_e$	The probability that two vehicles encounter at the exit
$P_b$	The random brake probability in the NS model
$S_{dyn}$	The fraction of dynamic drivers
$\beta$	The tunable parameter in the classical Fermi (CF) rule
$f_{c0}$	The initial fraction of cooperation (cooperator, C-agent) in the system
$f_{d0}$	The initial fraction of defection (defector, D-agent) in the system ( $= 1 - f_{c0}$ )
$f_c$	The fraction of cooperation in the system ( $N_c/N_{tot}$ ), $f_c(t=0) = f_{c0}$ (a.k.a. the frequency of cooperation or cooperation ratio)
$f_d$	The fraction of defection in the system ( $1 - f_c$ )
$P_{i,j \rightarrow j}$	The probability that an agent $i$ turns to an agent $j$ after it plays a game with an agent $j$
$U_i$	The real payoff of agent $i$ in the snowdrift game (SG) with the self-questioning Fermi (SQF) mechanism
$U'_i$	The virtual payoff of agent $i$ in the SG with the SQF mechanism

$\epsilon = \delta = 10^{-10}$ . Since  $\epsilon = \delta \ll 1$ , they do not really affect the payoff matrix but satisfy the payoff rank of the SG. The advanced characteristics that two parameters ( $\epsilon$  and  $\delta$ ) represent can be described as follows: (1) the vehicles leave the exit following the information feedback when cooperation takes place (indicated by the factor  $\epsilon$ ), (2) the defective penalty is imposed if both players choose to defect at the exit (implied by the factor  $\delta$ , see Sect. 2.4.2 for detail). Both scenarios contribute to the payoff matrix satisfying the inequalities (both  $2R > T + S$  and  $T > R > S > P$ ), which makes the evolutionary game unique in the ITS.

**Table 2** Payoff matrix of an evolutionary game

		Column	Player
		C	D
Row	C	R, R	S, T
Player	D	T, S	P, P
or equivalently			
		C	D
Row	C	R	S
Player	D	T	P

**Table 3** Payoff matrix of the SG

		Column	Player
		C	D
Row	C	$0.5 + \epsilon, 0.5 + \epsilon$	0, 1.0
Player	D	1.0, 0	$-\delta, -\delta$

The commonly used updating rules include the deterministic rule proposed by Nowak and May [41], the stochastic evolutionary rule proposed by Szabó and Tóke [47] and the memory-based self-questioning updating rule proposed by Wang et al. [55]. Later, Gao et al. [24] combined the self-questioning mechanism [55] with the stochastic Fermi rule [47]. In Gao et al. [24], they considered that players get real payoffs through a game on the basis of the payoff matrix in each time step. Meanwhile, each player calculates a virtual payoff by self-questioning, i.e., to adopt its anti-strategy and play a virtual game with its neighbors who keep their strategies unchanged, and get a virtual payoff. By comparing the real payoff and the virtual payoff, players will find out whether their current strategies are advantageous. In the next round, player will change its current strategy to its anti-strategy with probability  $P_{i,i' \rightarrow i'}$ :

$$P_{i,i' \rightarrow i'} = \frac{1}{1 + \exp[\beta(U_i - U'_i)]} \tag{1}$$

where  $U_i$  and  $U'_i$  are the real and virtual payoff of player  $i$ , respectively. The parameter  $1/\beta$  denotes the noise parameter modeling the uncertainty caused by strategy adoption. It is noteworthy that a player does not play a game with itself in the study of Gao et al. [24], while in the original work of Szabó and Tóke [47], the self-play, i.e., each player plays a game with itself is included. In the present work, we consider each player plays game with both itself and its neighbor. Based upon this self-play mechanism, we propose a modified SQF updating rule by redefining payoffs such that  $U_i$  and  $U'_i$  include the self-play payoffs as shown in the following table (Table 4, entries correspond to the row player’s payoffs).

**Table 4** The real and virtual payoffs in the SG with the SQF and the CF updating rules. The self-play is included in both cases. a and b indicate two examples of payoff calculations

	Real payoff <sup>c</sup> (SQF)		Virtual payoff (SQF)		Real payoff <sup>c</sup> (CF)	
	C	D	C	D	C	D
C	$1.0 + 2\epsilon$ <sup>a</sup>	$0.5 + \epsilon$	$1.0 - \delta$ <sup>b</sup>	$-2\delta$	$1.0 + 2\epsilon$	$0.5 + \epsilon$
D	$1.0 - \delta$	$-2\delta$	$1.0 + 2\epsilon$	$0.5 + \epsilon$	$1.0 - \delta$	$-2\delta$

<sup>a</sup> When a C-agent plays a game with its neighboring C-agent, each C-agent gets  $0.5 + \epsilon$  as the payoff. Meanwhile, the C-agent plays a game with itself and gets  $0.5 + \epsilon$  as the payoff. Therefore, the real payoff that a C-agent meets another C-agent in the SG with the SQF updating rule is equal to the sum of these two payoffs, i.e.,  $1.0 + 2\epsilon$ .

<sup>b</sup> When a C-agent plays a game with its neighboring C-agent, the virtual payoff is calculated as follows: the C-agent adopts its anti-strategy (D-agent) and plays a virtual game with its neighboring C-agent, the C-agent gets 1.0 as the payoff. Meanwhile, the C-agent adopts its anti-strategy (D-agent) and plays a game with itself with anti-strategy (also D-agent) and gets  $-\delta$  as the payoff. Therefore, the virtual payoff that a C-agent meets a C-agent in the SG with the SQF updating rule is equal to the sum of these two payoffs, i.e.,  $1.0 - \delta$ .

<sup>c</sup> The real payoff in the SG with the CF updating rule is the same as the real payoff in the SG with the SQF updating rule. Entries correspond to the row player's payoffs.

Unless noted otherwise the SQF rule hereafter refers to the modified SQF rule. For comparison, we also study the classical Fermi (CF) rule [47] case without employing the SQF mechanism, in which players update their strategies by learning from their neighbors, as the updating mechanism:

$$P_{i,j \rightarrow j} = \frac{1}{1 + \exp[\beta(U_i - U_j)]}. \quad (2)$$

where  $U_i$  and  $U_j$  are considered as real payoffs (including the self-play payoffs) of players  $i$  and  $j$  according to the payoff matrix shown above (also see Table 4). When a C-agent plays a game with another C-agent, the probability of a C-agent turns to a D-agent is  $P_{c,c \rightarrow d} = 1 - P_{c,c \rightarrow c}$ .

In this chapter, we study a 1-D ITS with dynamic periodic boundary conditions, which is different from the 2-D lattice case, in which each player usually has four nearest neighbors (i.e., von Neuman neighborhood). In the 2-D case, the players can randomly choose one of their immediate neighbors with equal probability and update their strategies by learning from their neighbors (i.e., with the CF updating rule). Each player will adopt the selected neighbor's strategy (C or D) with a certain probability  $P$  as shown in Eq. (2), which is usually determined by the payoffs of the two players. As the players aim at maximizing their own benefits, therefore, if the selected neighbor has a higher payoff, it is more likely that its strategy will be adopted, and vice versa [47]. Given the fact that two routes are separated in our model, the game can take place only at the 2-to-1 lane junction near the exit of each ITS pattern. Since cooperators and defectors initially are randomly distributed on each route, it is similar to the situation in which each player randomly chooses one of its immediate neighbors at the exit, as in the 2-D case.



The key quantity for characterizing the cooperative behavior is the frequency of cooperation  $f_c$ , which is defined as the fraction of cooperators in the whole population. The parameter  $f_c$  is obtained by counting the number of cooperators in the whole population ( $N_c/N_{tot}$ ) after the system reaches an equilibrium state, at which the number of cooperators fluctuates slightly around an average value. In our model, we assume that the initial fraction of cooperation is  $f_{c0}$  and defectors is  $f_{d0} = 1 - f_{c0}$ . Since we fix the total number of vehicles  $N_{tot}$  in the ITS, the fractions of cooperation,  $f_c(t)$ , and defection,  $f_d(t) = 1 - f_c(t)$ , evolve with time  $t$  when games take place at the exit.

### 2.3 The NS Mechanism

The Nagel-Schreckenberg (NS) model is briefly introduced as follows, which can be divided into the following four rules [39]:

R1: Acceleration:

$$v_i(t) \rightarrow v_i(t + \frac{1}{3}) = \min[v_i(t) + 1, v_{max}]; \quad (3)$$

R2: Deceleration:

$$v_i(t + \frac{1}{3}) \rightarrow v_i(t + \frac{2}{3}) = \min[v_i(t + \frac{1}{3}), g_i(t)]; \quad (4)$$

R3: Random brake:

$$v_i(t + \frac{2}{3}) \rightarrow v_i(t + 1) = \max[0, v_i(t + \frac{2}{3}) - 1]; \quad (5)$$

with a certain brake probability  $P_b$ ;

R4: Movement:

$$x_i(t + 1) = x_i(t) + v_i(t + 1). \quad (6)$$

In the NS model, the road is divided into cells (sites) with a length of  $\Delta x = 7.5\text{m}$ . The total length of the route is set to be  $L = 2,000$  cells (corresponding to 15 km).  $g_i(t)$  denotes the number of empty cells in front of car  $i$ , i.e., the gap or headway. A time step corresponds to  $\Delta t = 1\text{s}$ , the typical time a driver needs to react. In the present work, we set the maximum velocity  $v_{max} = 3$  cells/time step (corresponding to 81 km/h and thus is a reasonable value) for simplicity.

## 2.4 Two-Route Model and Exit Scenario

### 2.4.1 Two-Route Scenario

We adopt the modified version of the two-route model proposed by Wahle et al. [52]. We assume that the total number of cars in a 1-2-1 route ITS is  $N_{tot}$  that includes the waiting cars. To initialize the simulation, all vehicles wait on the lane before they enter the ITS. If a driver is a so-called dynamic one, he selects the route according to the real-time information displayed on the roadside, while a percentage of drivers (referred to as static drivers) ignores the advice, thus entering a route randomly. The length of two routes  $A$  and  $B$  are equal to each other. The fractions of dynamic and static travelers are  $S_{dyn}$  and  $1 - S_{dyn}$ , respectively. After a vehicle enters one of two routes, the vehicle follows the dynamics of the NS model. Since we use dynamic periodic boundary conditions, after a vehicle reaches the end point, it immediately returns to the waiting lane connected to the entrance with a position next to the waiting car in front of it without a gap. In other words, the dynamic periodic boundary conditions indicate that the waiting lane length is dynamic instead of static, which can only hold the number of waiting cars at the current moment. So we do not really care about the vehicle dynamic on the waiting lane. It is important to note that if a vehicle cannot enter the preferred route, it will wait till the next time step rather than entering the un-preferred route. In simulations, vehicles could enter the preferred route only when the first three sites (given  $v_{max} = 3$  cells/time step) of the route are empty in order to avoid collisions.

### 2.4.2 Exit Scenario

The dashed box in Fig. 2 illustrates the “one entrance and one exit” structure of the ITS. In reality, there are different paths for drivers to choose from one place to another. Different drivers departing from the same place could choose two different paths to get to the same destination, which is analogous to a 1-2-1 route system. The rules at the exit of the two-route system are as follows:

- (a) Rules at the exit when both vehicles have a chance to leave:
  - (i) According to the information shown on the information board 2 (see Fig. 2), the vehicle on the route with higher vehicle density leaves first;
  - (ii) If both routes have the same vehicle density, the vehicles leave randomly.
- (b) For the vehicles fail to leave at the exit, their position(t) = L and velocity (t) = position(t) – position(t – 1).

In 1-D and 2-D traffic flow models (see e.g., [43, 46]), when cooperations take place, the players have equal probability to move (1-D case) or move alternately (2-D case). However, in an ITS, when both players choose to cooperate, the

cooperators have a chance to follow the information shown on the board to leave the ITS. On the other hand, when both drivers choose to defect, both of them drive to position(t) = L with velocity(t) = 0 instead of velocity(t) = position(t) – position(t – 1) for penalty. In this way, the route conditions benefit from the cooperative behavior, and the defective penalty makes the defective behavior unfavorable. As we described earlier in this chapter, the influence is implied by the parameters  $\epsilon$  and  $\delta$  in the payoff matrix (Table 3), respectively. It is noteworthy that when the SG is not considered in Sect. 3.1, all the drivers are forced to follow the exit scenario, which is equivalent to the situation that all the players are assumed to be cooperators when adopting the SG. In reality, in order to impose all the drivers to follow the exit scenario, there must be automatic traffic barriers at the exit. However, it is impossible to have a barrier control at the end of each 2-to-1-lane junction in real traffic systems due to the high cost, which indicates the defector is highly likely to appear and thus the game analysis shown in Sect. 3.2 is more realistic compared to the case study in Sect. 3.1.

## 2.5 Related Definitions

The road conditions can be characterized by the fluxes of two routes, and the flux of the  $i$ th route is defined as follows:

$$F_i = V_{mean}^i \rho_i = V_{mean}^i \frac{N_i}{L_i} \quad (7)$$

where  $L_i$  represents the length of the  $i$ th route,  $V_{mean}^i$  and  $N_i$  denote the mean velocity of all the vehicles and the vehicle number on the  $i$ th route, respectively. The physical sense of the flux  $F$  is the number of vehicles passing the exit of the traffic system at each time step. Rather remarkably, the waiting cars do not contribute to the calculation of the time-dependent flux. Therefore the larger the value of  $F$  is, the better the processing capacity of the traffic system is. We describe four different feedback strategies as follows:

**MVFS:** At each time step, the velocity of each vehicle is known from navigation systems (GPS). The traffic control center calculates the mean velocity of each route and displays the number on the board located at the entrance of each route. Road users at the entrance will choose one road with a larger mean velocity.

**CCFS:** The position of each vehicle is known by the signal transmitted from navigation systems (GPS). The traffic control center computes the congestion coefficient of each route based on this information and displays it on the board. Road users at the entrance will choose the route with a smaller congestion coefficient. The congestion coefficient is defined as

$$C(t) = \sum_{j=1}^{q(t)} n_j^2(t). \quad (8)$$

Here,  $n_j(t)$  stands for vehicle number of the  $j$ th congestion cluster (see Fig. 2), in which cars are close to each other without a gap at time  $t$ .  $q(t)$  is the number of clusters on one route. However, it may not be optimal for road users to make a wise choice by considering only the current road condition. Given the situation that although initially  $V_{mean}^A < V_{mean}^B$ ,  $V_{mean}^A$  increases with time while  $V_{mean}^B$  decreases. In this circumstance, it is better for the road user to enter route  $A$  instead of route  $B$  since route  $A$  has the potential to become better. Based upon this scenario, we propose two concise and efficient feedback strategies as follows:

**MVDFS:** At each time step, each vehicle on the routes sends its velocity to the traffic control center. The work of the traffic control center is to calculate the velocity difference between time  $t_1$  and  $t_2$ , and display it on the board. Road users at the entrance will choose one road with a larger mean velocity difference.

The mean velocity difference ( $V_D$ ) between time  $t_1$  and  $t_2$  is defined as

$$\begin{aligned}
 V_D(t, \Delta t_v) &= V_{mean}(t_2) - |sgn(\Delta t_v)| \times V_{mean}(t_1) \\
 &= V_{mean}[t - (1 - H(\Delta t_v))\Delta t_v] - |sgn(\Delta t_v)| \times V_{mean}[t - H(\Delta t_v)\Delta t_v] \\
 &= \frac{\sum_{i=1}^{N(t_2)} V_i[t - (1 - H(\Delta t_v))\Delta t_v]}{N[t - (1 - H(\Delta t_v))\Delta t_v]} \\
 &\quad - |sgn(\Delta t_v)| \times \frac{\sum_{i=1}^{N(t_1)} V_i[t - H(\Delta t_v)\Delta t_v]}{N[t - H(\Delta t_v)\Delta t_v]}.
 \end{aligned} \tag{9}$$

where  $sgn(x)$  is the signum function of a real number  $x$ , which is defined as follows:

$$sgn(x) = \begin{cases} 1, & \text{if } x > 0 \\ 0, & \text{if } x = 0 \\ -1, & \text{if } x < 0 \end{cases} \tag{10}$$

and  $H(x)$  is the unit step function, which defined as the integral of the Dirac delta function:

$$H(x) = \int_{-\infty}^x \delta(s) ds = \begin{cases} 1, & \text{if } x \geq 0 \\ 0, & \text{if } x < 0 \end{cases} \tag{11}$$

$V_i(t)$  stands for the velocity of the  $i$ th vehicle at time  $t$ ,  $N(t)$  denotes the vehicle number on one route at time  $t$ ,  $t_2 = t - (1 - H(\Delta t_v))\Delta t_v$  and  $t_1 = t - H(\Delta t_v)\Delta t_v$ . It is noteworthy that for  $\Delta t_v = 0$ , MVDFS changes back to MVFS.

**CCDFS:** At each time step, the traffic control center receives data from the navigation systems (GPS) as CCFS. The work of the traffic control center is to calculate the congestion coefficient difference between time  $t_1$  and  $t_2$  and display it

on the board. Road users at the entrance choose one road with smaller congestion coefficient difference.

The congestion coefficient difference ( $C_D$ ) between time  $t_1$  and  $t_2$  is defined as

$$\begin{aligned}
 C_D(t, \Delta t_c) &= C(t_2) - |\text{sgn}(\Delta t_c)| \times C(t_1) \\
 &= C[t - (1 - H(\Delta t_c))\Delta t_c] - |\text{sgn}(\Delta t_c)| \times C[t - H(\Delta t_c)\Delta t_c] \\
 &= \sum_{j=1}^{q(t_2)} n_j^2 [t - (1 - H(\Delta t_c))\Delta t_c] \\
 &\quad - |\text{sgn}(\Delta t_c)| \times \sum_{j=1}^{q(t_1)} n_j^2 [t - H(\Delta t_c)\Delta t_c].
 \end{aligned} \tag{12}$$

where the definitions of  $n_j(t)$  and  $q(t)$  are the same as those defined in CCFS. Similar to MVDFS, when  $\Delta t_c = 0$ , CCDFS returns to CCFS. Given the implementation efficiency in real traffic systems, we only focus on the situations that  $\Delta t_{v,c} > 0$ , but Eqs. (9 and 12) are valid for any real number of  $\Delta t_{v,c}$ .

Finally, we point out that initially we set the routes and information boards empty and let vehicles enter the routes randomly during the first 100 time steps in the simulation. Thus, the information feedback starts at the 101th time step. In the following section, the performance of four different feedback strategies will be shown and discussed in detail.

### 3 Simulation Results

#### 3.1 Advanced Information Feedback in a 1-2-1 Route ITS

Firstly, we focus on the advanced information feedback strategy in ITSs itself, thus ignoring the evolutionary game in this section. Given the stability and convergency, the smoothed simulation results shown in Fig. 3 are obtained based on 10 times average over 90,000–100,000 time steps. Figures 3a, b show the dependence of the average flux on the time difference  $\Delta t_c$  and  $\Delta t_v$  by using CCDFS and MVDFS, respectively. As to the routes' processing capacity, there are positive peak structures, corresponding to the highest flux  $\sim 0.43$  in both cases, at the vicinity of  $\Delta t_c \approx 2$  and  $\Delta t_v \approx 3$ . We also test the simulation result without 10-time average, which basically shows the same curve shape and the peak location. Therefore, the average does not change the result to any significant degree. When  $\Delta t_v = 0$  ( $\Delta t_c = 0$ ), MVDFS (CCDFS) is equivalent to MVFS (CCFS), which allows direct comparison between MVDFS (CCDFS) and MVFS (CCFS). In Fig. 3, it is clear that both MVDFS and CCDFS significantly improve the road capacity compared to the previous strategies when the time difference is less than  $\sim 30$ . Supposing if we delete signum function,  $\text{sgn}(x)$ , in Eqs. (9–12), when  $\Delta t_v = 0$  ( $\Delta t_c = 0$ ),  $V_D(t, \Delta t_v) = 0$  ( $C_D(t, \Delta t_c) = 0$ ),

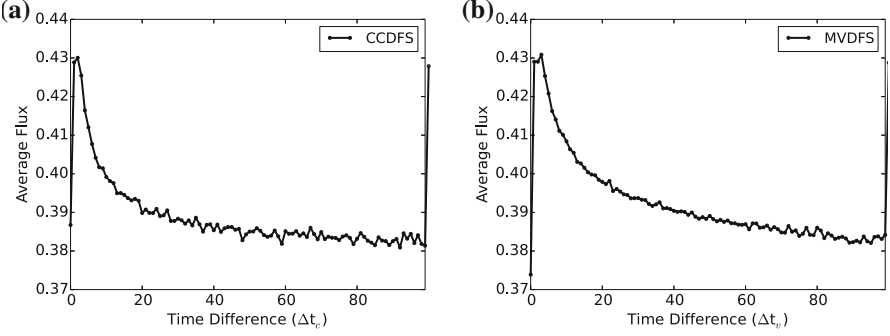


**Fig. 3** **a** Average flux by performing CCDFS versus time difference  $\Delta t_c$ . **b** Average flux by performing MVDFS versus time difference  $\Delta t_v$ . The results are based on 10 times average. The parameters are,  $S_{dyn} = 1.0$ , and  $N_{tot} = 2,000$

i.e., the random case, then we cannot intuitively see the difference between the improved strategies and previous ones in Fig. 3. Unless noted otherwise, all the parameters hereafter refer to  $L_A = L_B = 2,000$ ,  $P_b = 0.25$ ,  $S_{dyn} = 1.0$ ,  $\Delta t_c = 2$ ,  $\Delta t_v = 3$ , and  $N_{tot} = 2000$ .

In contrast to MVDFS and CCDFS, the fluxes of two routes adopting MVFS and CCFS show larger oscillations (see Fig. 4). These oscillations could be caused by several factors. First, as we have mentioned earlier, the NS model has a random brake scenario which causes the fragile stability of velocity, thus MVFS cannot completely reflect the real route conditions. Second, the oscillations can be partially caused by the potential information lag by using the current information [54]. When we adopt MVDFS or CCDFS, it is similar to the situation in which we implement a linear extrapolation in time and therefore it is equivalent to the prediction feedback [15, 19] for a short time scale to a certain degree. Though CCFS is better than MVFS, both MVFS and CCFS cannot reflect the tendency of road condition variation with time. For example, when adopting MVDFS, if there exist congestion clusters at the end of route A, the average velocity of the whole route will definitely decrease even though  $V_{mean}^A > V_{mean}^B$ . The mean velocity difference of route A,  $V_D^A(t, \Delta t_v)$ , is negative [see Eq. (9)] in this situation. If a road user finally chooses to enter route B, there are three possible outputs: first,  $V_{mean}^B(t_2) > V_{mean}^B(t_1)$ , with  $t_2 > t_1$ ; second,  $V_{mean}^B$  remains the same; third,  $V_{mean}^B$  decreases but  $V_D^B(t, \Delta t_v) > V_D^A(t, \Delta t_v)$  (both of them are negative under this circumstance). In order to prevent the congestion clusters from further expanding, the route users should enter route B whose condition tends to be better (condition I) or no worse than that of route A (condition II or III). For CCDFS, the analysis is similar. The only difference is that road users will select the route with smaller congestion coefficient difference  $C_D(t, \Delta t_c)$  instead, because the large congestion coefficient indicates the unfavorable jammed states which certainly do harm to the traffic system. Compared with MVFS and CCFS, the performance by adopting MVDFS and CCDFS is remarkably improved, not only considering the value but also

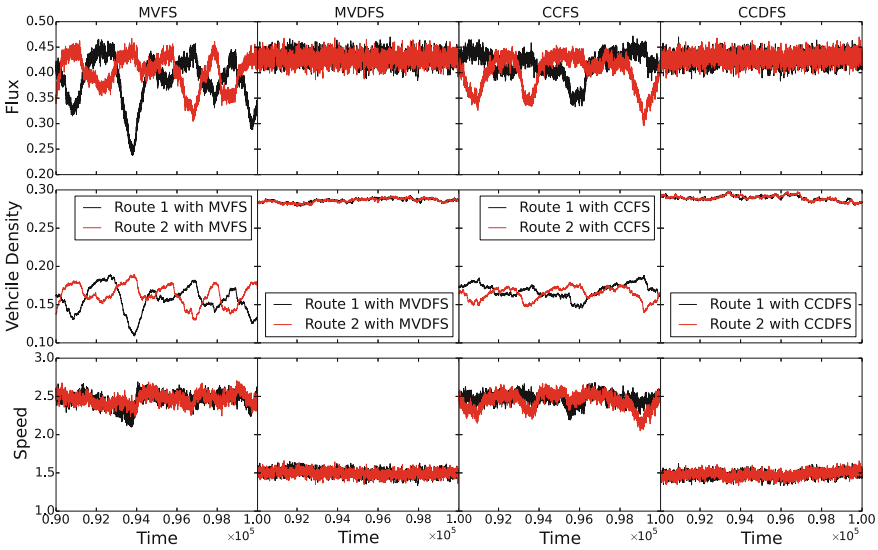


**Fig. 4** Flux (the *first row*), vehicle density (the *second row*), and average speed (the *third row*) of each route with mean velocity feedback strategy (MVFS, the *first column*), mean velocity difference feedback strategy (MVDFS, the *second column*), congestion coefficient feedback strategy (CCFS, the *third column*), and congestion coefficient difference feedback strategy (CCDFS, the *fourth column*).  $S_{dyn} = 0.5$

the stability of the flux. Therefore, considering the flux of the two-route system, MVDFS and CCDFS are better.

In Fig. 4, the plot of vehicle density versus time step shows a similar tendency as that of the flux. The routes' accommodating capacity is greatly enhanced with an increase in the average vehicle density from 0.16 to 0.29, thus the high fluxes of two routes with MVDFS and CCDFS are mainly due to the increase of the vehicle density. According to the stability of the vehicle density on each route, the vehicles are uniformly distributed on each route instead of staying together at the end of the route. The plot of speed versus time step shows that although the velocities are more stable by using the new strategies, they are lower than MVFS and CCFS. The reason is that the routes' accommodating capacity is more efficient by using the new strategies. As mentioned earlier, the system has only one exit, and at most one car can leave at each time step. Therefore the more cars the lane holds, the lower velocities the vehicles have. Fortunately, the traffic flux consists of two parts, the mean velocity and the vehicle density. Hence as long as the vehicle density,  $\rho = N/L$ , is large enough, the road flux can still be greatly improved.

Figure 5 shows the dependence of the average flux fluctuates on the fraction of dynamic travelers ( $S_{dyn}$ ) by using four different feedback strategies. As to the routes' processing capacity, the new strategies are proved to be better than the

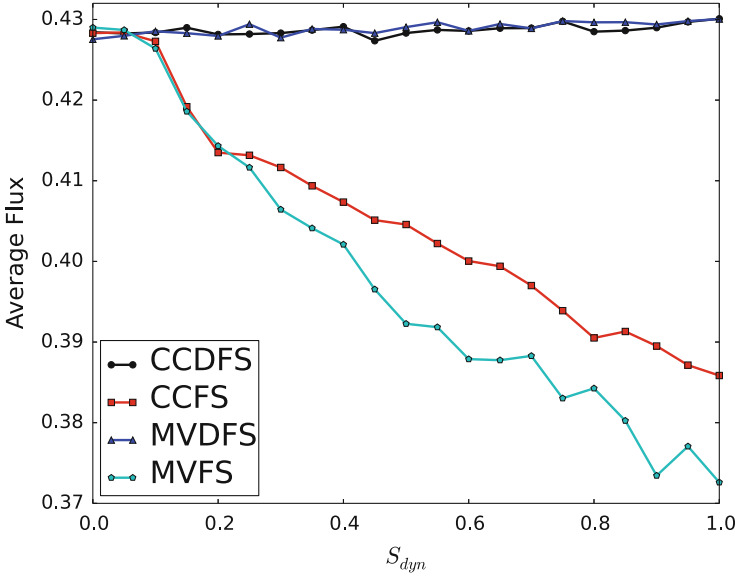


**Fig. 5** Average flux by performing different strategies versus  $S_{dyn}$

previous ones because the fluxes are always larger at each  $S_{dyn}$  value and even slightly increase with a persisting increase of dynamic drivers. The fact that the values of average fluxes in Fig. 5 by adopting MVFS and CCFS are smaller than those shown in [54] is caused by the different structures of the (1-2-1 route) traffic system and the exit scenario.

Finally, it is of particular interest to find that the newly proposed information feedback strategy seems to be independent of the selected information type and only relies on the information changing rate or tendency. Without loss of generality, we focus on the comparison of CCFS and CCDFS in the following section and set  $\Delta t_c = 2$  for all cases.

### 3.2 Evolutionary Game Coupled with the NS Model in a 1-2-1 Route ITS

In this section, we focus on the evolutionary game coupled with the NS model in a 1-2-1 route ITS. The simulations are carried out for 200,000 time steps. The results shown in Figs. 6 and 7 are based on the average over 190,000–200,000 time steps. As will be shown later (e.g., see Fig. 8), the evolution of cooperation reaches a steady state at around 20,000 time step. Since the calculated result does not vary a lot after it reaches the steady state, the total run time steps only need to reach greater than 20,000. If a vehicle passes the exit without encountering any vehicle on the



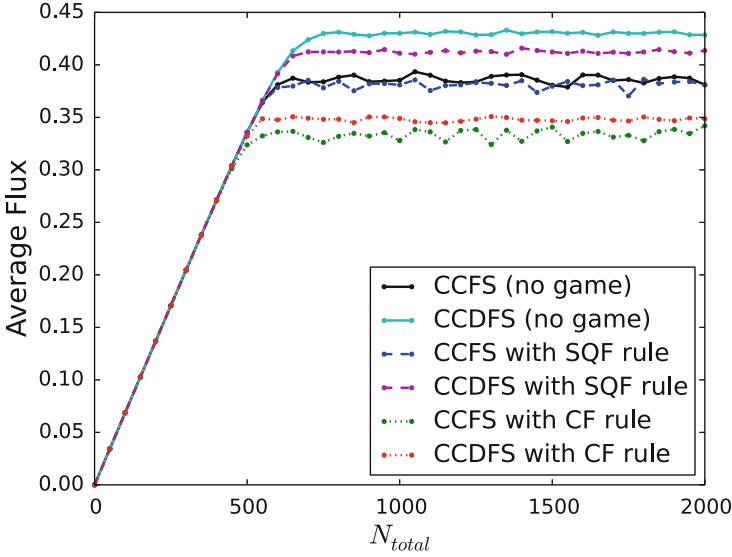


**Fig. 6** Average flux versus total number of vehicles ( $N_{tot}$ ) in the traffic system

alternative route, it leaves the system without changing its strategy (i.e., C-agent or D-agent). If the vehicles near the exit on both routes have a chance to leave the system, the game takes place and the players update their strategies based upon the rules described in Sect. 2.2. Once a car leaves the system, it keeps its strategy until the driver has a chance to play a game with others at the exit again, and so on and so forth.

As we described earlier, we employ the Snowdrift Game (SG) [45] in this chapter. We first investigate the dependence of the average flux on the total vehicle number,  $N_{tot}$ , in an ITS by adopting CCFS (without the SG), CCDFS (without the SG) and CCDFS coupled with the SG (with both the self-questioning Fermi (SQF) updating rule and the classical Fermi (CF) updating rule). In Fig. 6, the solid lines with different colors show the cases without adopting the SG. The dashed lines with different colors illustrate the cases with the SQF updating rule [see Eq. (1)] and the dotted lines with different colors represent the cases with the CF updating rule [see Eq. (2)]. It is clear that CCDFS without adopting the SG has the highest flux among all six cases. Given the payoff matrix (Table 3) and the fact that when the SG is not adopted, all the drivers are forced to be cooperators due to the fictitious barrier control at the exit, this result is within our expectation. However, the game analysis in this section is more realistic in a real traffic system as explained in Sect. 2.4.2. When adopting the SG, the saturated  $N_{tot}$  decreases with respect to the cases without evolutionary game, consistent with the result shown in Fig. 2 in Perc [43]; the evolutionary game has a tendency to make the road saturated (in our case) or phase state transition from free flow to fully jammed flow (in 2-D BML model [43]) occurring at a relatively low density state. Compared with the CCDFS case with the

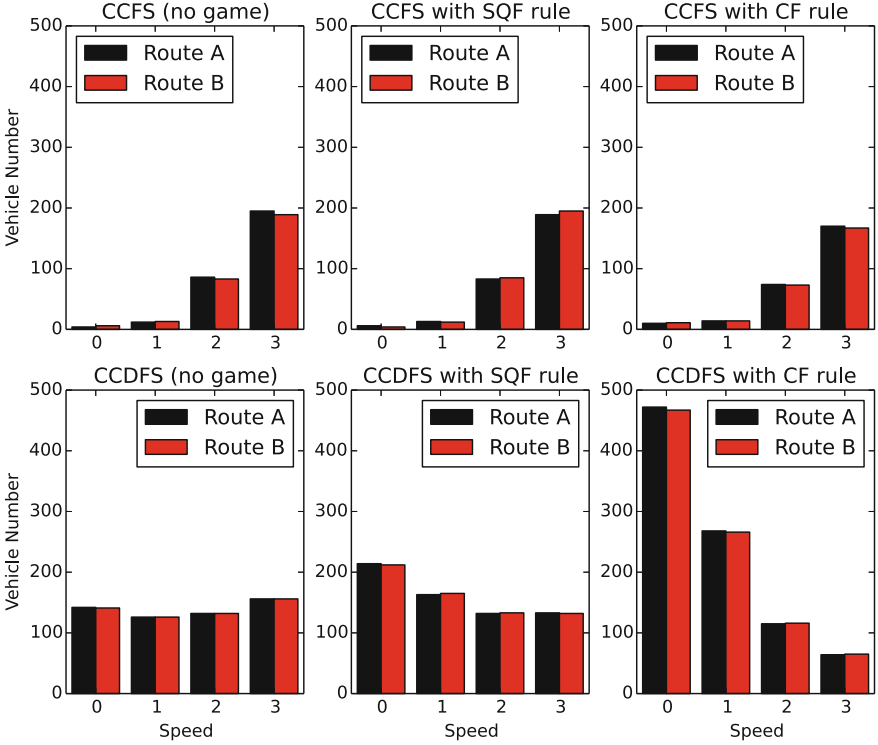


**Fig. 7** The velocity distribution of each route with CCFS (the *first row*) and CCDFS (the *second row*). The *first column* shows the cases without adopting the SG. The *second and third columns* illustrate the velocity distribution from the information feedback coupled with the SG (the *second column*: with the SQF updating rule; the *third column*: with the CF updating rule)

CF rule (the red dotted line), the average flux by adopting CCDFS with the SQF rule (the magenta dashed line) is higher, indicating that the SQF rule is more favorable in terms of alleviating the traffic congestion. As expected from the earlier analysis, the worst condition occurs at the situation by adopting CCFS with the CF updating rule (the green dotted line), which corresponds to the lowest average flux and the smallest saturated vehicle density. In the following analysis of the evolutionary game, we focus on the strategy CCDFS with both the SQF and the CF updating rules. We select two values of  $N_{tot} = 200$  (unsaturated state) and  $N_{tot} = 2,000$  (fully saturated state) as case studies. Hereafter unless noted otherwise, we choose  $f_{c0} = 0.85$  and  $\beta = 10$  in this section.

Figure 7 shows the the velocity distribution of each route with and without the evolutionary game. When adopting the SG, the fraction of low speed vehicles clearly increases with respect to the cases without the SG. Compared with the cases adopting the SQF updating rule, the CF updating rule leads to a relatively large fraction of low speed vehicles (especially for the combination of CCDFS with the

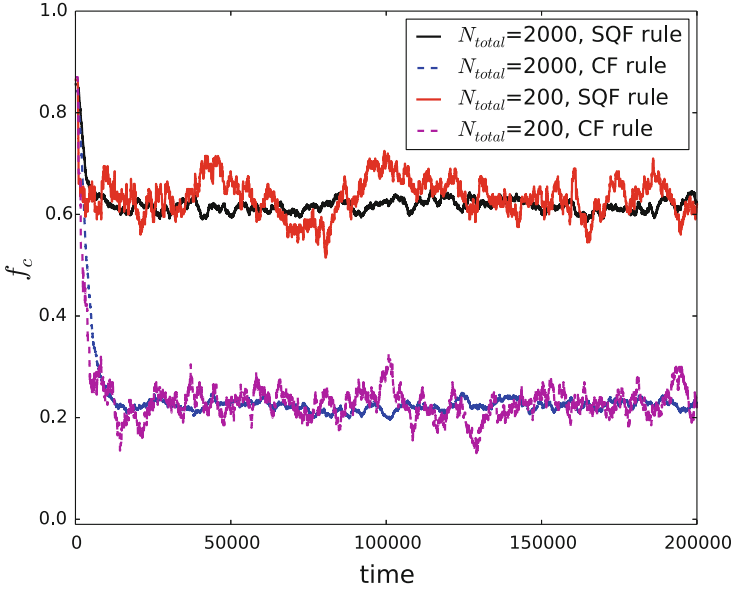


**Fig. 8** Fraction of cooperation versus time by adopting CCDFS

CF rule), which indicates an unfavorable jammed state on the route. The payoff matrix (Table 3) indicates that the traffic congestion is mainly caused by the defective behavior of D-agents at the end of each route. Thus, the SQF updating rule is better than the CF updating rule in terms of alleviating the traffic congestion. The detailed analysis of the evolutionary game below will help one further understand the vehicle dynamic behavior shown above.

We first investigate the evolution of cooperation with the classical Fermi (CF) and the self-questioning Fermi (SQF) rule (see Sect. 2.2 for detail). Figure 8 shows the variation of the fraction of cooperation,  $f_c$ , with time based on different updating rules and total vehicle number,  $N_{tot}$ . It shows that the evolution of cooperation reaches a steady state at around 20,000 time steps. In both cases, the fraction of cooperation,  $f_c$ , reaches an equilibrium state with the density of cooperators fluctuating slightly around a convergent value. Although the convergent value with the SQF mechanism is higher than that with the CF mechanism, it is independent of the vehicle number or the phase state in both cases. When  $N_{tot} = 200$ , it converges faster than the larger  $N_{tot} = 2,000$  case. Inspection of Fig. 8 reveals that the SQF mechanism can prevent the system from being enmeshed in a globally defective trap, which is a shortcoming of the existing models based on the learning mechanisms. The underlying reason lies in the fact that the players with the SQF mechanism consider both the real and virtual payoffs by playing games with themselves and their neighbors, depending on which players make their decisions on whether switching to their anti-strategy. In contrast to the case with the SQF rule, the players with the CF rule only consider the real payoffs without self-questioning, so they cannot further consider the information about their

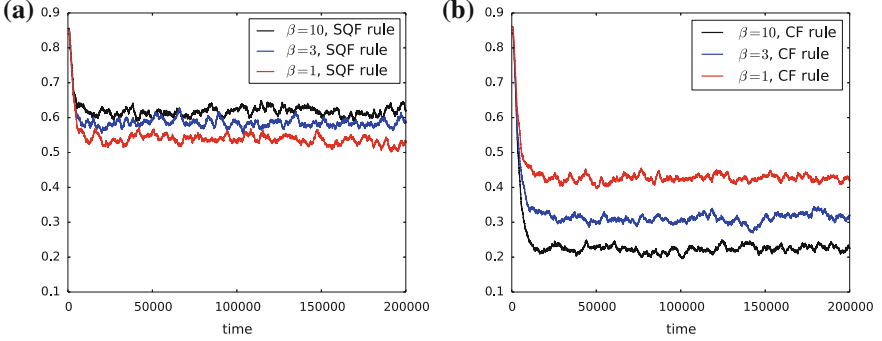


**Fig. 9** Fraction of cooperation  $f_c$  versus time for different values of  $\beta$  by adopting CCDFS

surroundings and the mutual payoffs of the whole system. This leads to a higher possibility of selfish individuals trying to maximize their own benefit to grow in the system. The relatively low flux (Fig. 6) and large fraction of low speed vehicles (Fig. 7) with the CF rule can therefore be explained by the low fraction of C-agent in the system.

In order to show the advantages of the SQF mechanism, we also study the dependence of the updating mechanism on the value of  $\beta$ , which characterizes the noise introduced to permit irrational choices. Figure 9 shows the variation of the cooperation fraction,  $f_c$ , with time by adopting the SQF and the CF updating rules based on various  $\beta$ . We select  $\beta = 1, 3, 10$  as case studies. It is of particular interest to find that the convergent value of  $f_c^{SQF}$  in the newly proposed SQF mechanism only slightly relies on the tunable parameter  $\beta$ ; a large  $\beta$  corresponds to a slightly large  $f_c^{SQF}$ . With the CF mechanism, the convergent value of  $f_c^{CF}$  however, greatly relies on the noise term  $\beta$ ; the larger the  $\beta$ , the smaller the convergent  $f_c$ . On average,  $f_c^{SQF} > f_c^{CF}$ . This comparison intuitively reveals one of the advantages of the SQF mechanism.

We also study the effect of the initial cooperation fraction,  $f_{c0}$ , on the convergent value of  $f_c$  by adopting the SQF and the CF rules. Figure 10 shows five cases with initial cooperation ratios  $f_{c0} = 1.0, 0.85, 0.63, 0.23$  and  $0.05$  by adopting the SQF (Fig. 10a) and CF (Fig. 10b) rules. Despite the different initial cooperation ratios,  $f_{c0}$ , they all converge to the same steady state,  $f_c \approx 0.63$  (for SQF) and  $0.23$  (for CF). Interestingly, the convergent value is independent of the initial fraction,  $f_{c0}$ , in both cases. We also test the case of the CF rule without self-play payoff counted, the convergent value is also independent of  $f_{c0}$ . The convergent  $f_c$  with the SQF rule is always higher than that with the CF rule at various  $f_{c0}$  in Fig. 10. Again, it demonstrates the advantages of the newly proposed SQF mechanism. The simulation results with original SQF rule [24] adopted are not shown as it is even worse than the CF rules in terms of the convergent  $f_c$  under certain circumstances. It seems to be caused by the 1-D structure of our model, where each player at most has one neighbor whereas in a 2-D lattice, each player can have 4 neighbors or 8 neighbors.

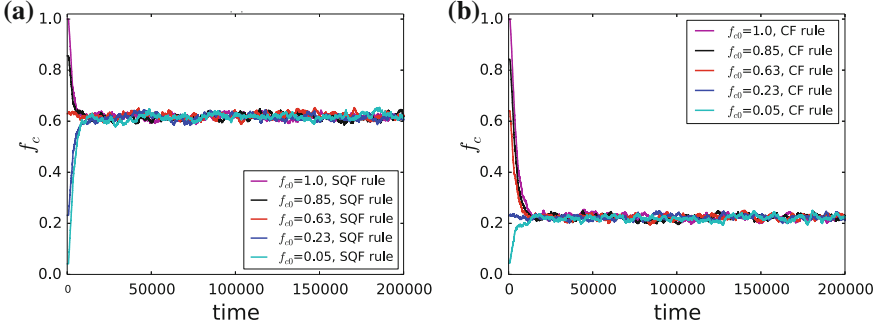


**Fig. 10** Fraction of cooperation  $f_c$  versus time at various  $f_{c0}$  by adopting CCDFS

However, the self-play [47] solves the shortcoming of the original SQF rule. By all accounts, the improved SQF mechanism will be a powerful tool in the analysis of evolutionary game in both traffic networks and other social and economic systems.

Finally, we analytically calculate the evolution of the cooperation ratio,  $f_c$ , by using a simple mean-field approximation [4, 46]. In the SG with either the SQF or CF updating rule [see Eqs. (1–2)], if one agent is cooperator and the other is defector (ignoring the parameter  $\epsilon$  and  $\delta$  here due to their tiny values), then

$$P_{c,d \rightarrow d}^{SQF} = \frac{1}{1 + e^{0.5\beta}}; P_{c,d \rightarrow d}^{CF} = \frac{1}{1 + e^{-0.5\beta}} \quad (13)$$

$$P_{d,c \rightarrow c}^{SQF} = 0.5; P_{d,c \rightarrow c}^{CF} = \frac{1}{1 + e^{0.5\beta}} \quad (14)$$

If both agents are defectors, then

$$P_{d,d \rightarrow c}^{SQF} = \frac{1}{1 + e^{-0.5\beta}}; P_{d,d \rightarrow c}^{CF} = 0.5 \quad (15)$$

If both agents are cooperators:

$$P_{c,c \rightarrow d}^{SQF} = 0.5; P_{c,c \rightarrow d}^{CF} = 0.5 \quad (16)$$

As  $f_c + f_d = 1$ , the mean-field equation can be written as an equation about  $f_c$  as follows (we choose the situation of the SG with the SQF updating rule as an example of analysis):

$$\begin{aligned} \frac{df_c}{dt} &= P_e \times \left( 2f_c \cdot f_d \left( P_{d,c \rightarrow c}^{SQF} - P_{c,d \rightarrow d}^{SQF} \right) + f_d \cdot f_d \left( P_{d,d \rightarrow c}^{SQF} + P_{d,d \rightarrow c}^{SQF} \right) + f_c \cdot f_c \left( -P_{c,c \rightarrow d}^{SQF} - P_{c,c \rightarrow d}^{SQF} \right) \right) \\ &= P_e \times \left( 2f_c \cdot f_d \left( 0.5 - \frac{1}{1 + e^{0.5\beta}} \right) + f_d \cdot f_d \frac{2}{1 + e^{-0.5\beta}} - f_c \cdot f_c \right) \end{aligned} \quad (17)$$

**Table 5** Comparison of the convergent value of  $f_c$  by adopting the mean-field approximation and the simulation results in the SG with the SQF and CF updating rules

	$\beta = 1$ (MFA <sup>a</sup> )	$\beta = 1$ (SIM <sup>b</sup> )	$\beta = 3$ (MFA)	$\beta = 3$ (SIM)	$\beta = 10$ (MFA)	$\beta = 10$ (SIM)
Convergent $f_c^{SQF}$	0.55	0.54	0.62	0.59	0.67	0.63
Convergent $f_c^{CF}$	0.44	0.43	0.35	0.32	0.29	0.23

<sup>a</sup> MFA mean-field approximation<sup>b</sup> SIM simulation

where  $P_e$  is the probability that two cars encounter at the exit (so the SG takes place) before leaving an ITS. By either integrating Eq. (17) and assuming  $t \rightarrow \infty$ , or just assuming  $df_c/dt = 0$ , the analytic approximation of the steady state value,  $f_c$  can be obtained and compared with the corresponding simulation result (Table 5). Table 5 shows that our simulation results are in good agreement with the analytic solution from the mean-field approximation, especially when  $\beta$  is relatively small, e.g.,  $\beta = 1$ .

Finally, we point out that a lot of further studies are needed, involving the study of, e.g., player cooperative behavior by using the SG/PDG in an asymmetric two-route ITS with a speed limit bottleneck on the short route (e.g., see Fig. 1 in Chen et al. [9]). This study will allow us to investigate the cases with accidents. Also, it would be interesting to study the cooperative behavior by a n-person chicken game (e.g., see [48]) when games take place at the end of a multi-route intelligent transportation system (e.g., see Fig. 1 in Dong et al. [19]). Moreover, an optimal exit scenario proposal may have a chance to increase both the fraction of cooperation and the vehicle flux.

## 4 Conclusion

For the first time, we studied the advanced information feedback coupled with an evolutionary game in a 1-2-1 route ITS with dynamic periodic boundary conditions. The feedback information makes the cooperative behavior unique in ITSs. When a cooperation takes place, the cooperator leaves the exit by following the information feedback shown on the board. We studied in detail the evolution of cooperation for the Snowdrift Game (SG) model with two different updating rules: an improved self-questioning Fermi (SQF) mechanism and the classical Fermi (CF) mechanism. The former one shows several advantages compared with the latter one. Note that in our model, each player not only plays game with its neighbor but also with itself, thus including the self-play payoffs. The SQF mechanism avoids the system from being enmeshed in a trap of the globally defective state, which is a shortcoming of the pre-existing models. Furthermore, we investigated the influences of total

number of vehicles in an ITS, noise term, and the initial fraction of cooperation on the SG. The results show that the steady state of the cooperation ratio,  $f_c$ , is independent with the total number of vehicles and the initial fraction of cooperation. Compared with the CF rule, the convergent values of  $f_c$  with the SQF rule are barely affected by the noise term and show relatively a higher steady cooperation ratio  $f_c$ . Our simulation results are in good agreement with the analytic solutions derived from the mean-field approximation and therefore shed new light on the study of evolutionary games in 1-D intelligent traffic networks.

In addition, the simulation results (without adopting the SG) with four different feedback strategies, i.e., MVFS, CCFS, MVDFS, and CCDFS in a 1-2-1 route ITS, were compared in terms of variations of the flux, vehicle density, speed, and average flux against the fraction of dynamic drivers. Variations of average flux with time difference ( $\Delta t$ ) by adopting CCDFS and MVDFS indicate that MVDFS and CCDFS are better than the other two feedback strategies in an ITS with only one entrance and one exit. One highlight of this chapter is that it brings forward two new quantities, mean velocity difference and congestion coefficient difference, to radically improve road conditions. In contrast to the previous two feedback strategies, MVDFS and CCDFS can significantly improve the road conditions, in terms of increasing vehicle density and flux, reducing oscillation, and enhancing average flux with the increase of dynamic driver percentage. These advantages result from the fact that the new feedback strategies consider the tendency of road condition variations. Thus, in these situations, the system has the ability to alleviate the negative effects of congestion caused by the traffic jam. Thanks to the rapid development of modern scientific technology, MVDFS or CCDFS can be implemented in real traffic systems in the near future. If a navigation system (GPS) is installed in each vehicle, the velocity and position information of vehicles are known. Consequently, the mean velocity difference or the congestion coefficient difference in MVDFS or CCDFS can be calculated by the computers used to calculate the average velocity or congestion coefficient in previous strategies without extra cost. Taking into account the reasonable cost and more accurate description of road conditions, we conclude that these two feedback strategies are applicable.

**Acknowledgments** C.F. Dong appreciates many fruitful discussions with Prof. Bing-Hong Wang at the University of Science and Technology of China, and Dr. Nan Liu at the University of Chicago. The authors would like to thank the editors and the anonymous referees' helpful comments and suggestions.

## References

1. Adler JL, Blue VJ (1998) Toward the design of intelligent traveler information systems. *Transp Res Part C* 6:157–172
2. Axelrod R (1984) *The evolution of cooperation*. Basic books, New York
3. Axelrod R, Hamilton WD (1981) The evolution of cooperation. *Science* 211:1390–1396

4. Barato AC, Hinrichsen H (2008) Boundary-induced nonequilibrium phase transition into an absorbing state. *Phys Rev Lett* 100:165701
5. Barlovic R, Santen L, Schadschneider A, Schreckenberg M (1998) Metastable states in cellular automata for traffic flow. *Eur Phys J B* 5:793–800
6. Bellouquid A, Delitala M (2011) Asymptotic limits of a discrete kinetic theory model of vehicular traffic. *Appl Math Lett* 24:149–155
7. Bier VM, Hausken K (2013) Defending and attacking a network of two arcs subject to traffic congestion. *Reliab Eng Syst Saf* 112:214–224
8. Biham O, Alan Middleton A, Levine D (1992) Self-organization and a dynamical transition in traffic-flow models. *Phys Rev A* 46:R6124
9. Chen BK, Sun XY, Wei H, Dong CF, Wang BH (2011) Piecewise function feedback strategy in intelligent traffic systems with a speed limit bottleneck. *Int J Mod Phys C* 22:849–860
10. Chen BK, Sun XY, Wei H, Dong CF, Wang BH (2012) A comprehensive study of advanced information feedbacks in real-time intelligent transportation systems. *Phys A* 391:2730–2739
11. Chen BK, Dong CF, Liu YK, Tong W, Zhang WY, Liu J, Wang BH (2012) Real-time information feedback based on a sharp decay weighted function. *Comput Phys Commun* 183:2081–2088
12. Chowdhury D, Santen L, Schadschneider A (2000) Statistical physics of vehicular traffic and some related systems. *Phys Rep* 329:199–329
13. Colman AM (1995) *Game theory and its applications in the social and biological sciences*. Butterworth-Heinemann, Oxford
14. Dong CF (2009) News story: intelligent traffic system predicts future traffic flow on multiple roads. [PHYSorg.com](http://PHYSorg.com). 12 Oct 2009
15. Dong CF, Ma X, Wang GW, Sun XY, Wang BH (2009) Prediction feedback in intelligent transportation systems. *Phys A* 388:4651–4657
16. Dong CF, Ma X (2010) Corresponding angle feedback in an innovative weighted transportation system. *Phys Lett A* 374:2417–2423
17. Dong CF, Ma X, Wang BH (2010) Weighted congestion coefficient feedback in intelligent transportation systems. *Phys Lett A* 374:1326–1331
18. Dong CF, Ma X, Wang BH (2010) Effects of vehicle number feedback in multi-route intelligent traffic systems. *Int J Mod Phys C* 21:1081–1093
19. Dong CF, Ma X, Wang BH, Sun XY (2010) Effects of prediction feedback in multi-route intelligent transportation systems. *Phys A* 389:3274–3281
20. Dong CF, Paty CS (2011) Application of adaptive weights to intelligent information systems: an intelligent transportation system as a case study. *Inf Sci* 181:5042–5052
21. Dong CF, Wang BH (2011) Applications of cellular automaton model to advanced information feedback in intelligent traffic systems. In: Salcido A (ed) *Cellular automata—simplicity behind complexity*, pp 237–258. ISBN 978-953-307-579-2
22. Dong CF, Ma X (2012) Dynamic weight in intelligent transportation systems: a comparison based on two exit scenarios. *Phys A* 391:2712–2719
23. Fukui M, Nishinari K, Yokoya Y, Ishibashi Y (2009) Effect of real-time information upon traffic flows on crossing roads. *Phys A* 388:1207–1212
24. Gao K, Wang WX, Wang BH (2007) Self-questioning games and ping-pong effect in the BA network. *Phys A* 380:528–538
25. Gazis DC, Herman R, Rothery RW (1961) Nonlinear follow-the-leader models of traffic flow. *Oper Res* 9:545–567
26. Hao QY, Jiang R, Hu MB, Jia B, Wu QS (2011) Pedestrian flow dynamics in a lattice gas model coupled with an evolutionary game. *Phys Rev E* 84:036107
27. He ZB, Chen BK, Jia N, Guan W, Lin BC, Wang BH (2014) Route guidance strategies revisited: comparison and evaluation in an asymmetric two-route traffic network. *Int J Mod Phys C* 25:1450005
28. Helbing D (2001) Traffic and related self-driven many-particle systems. *Rev Mod Phys* 73:1067–1141



29. Helbing D, Treiber M (1998) Gas-kinetic-based traffic model explaining observed hysteretic phase transition. *Phys Rev Lett* 81:3042–3045
30. Hino Y, Nagatani T (2014) Effect of bottleneck on route choice in two-route traffic system with real-time information. *Phys A* 395:425–433
31. Hofbauer J, Sigmund K (1998) *Evolutionary games and population dynamics*. Cambridge University Press, Cambridge
32. Kerner BS, Konhäuser P (1994) Structure and parameters of clusters in traffic flow. *Phys Rev E* 50:54–83
33. Kerner BS (2011) Optimum principle for a vehicular traffic network: minimum probability of congestion. *J. Phys. A* 44:092001
34. Laval JA, Leclercq L (2010) Mechanism to describe stop-and-go waves: a mechanism to describe the formation and propagation of stop-and-go waves in congested freeway traffic. *Phil Trans R Soc A* 368:4519
35. Lee K, Hui PM, Wang BH, Johnson NF (2001) Effects of announcing global information in a two-route traffic flow model. *J Phys Soc Jpn* 70:3507–3510
36. Li XB, Wu QS, Jiang R (2001) Cellular automaton model considering the velocity effect of a car on the successive car. *Phys Rev E* 64:066128
37. Li RH, Yu JX, Lin J (2013) Evolution of cooperation in spatial Traveler’s Dilemma game. *PLoS ONE* 8:e58597
38. Nagatani T (2002) The physics of traffic jams. *Rep Prog Phys* 65:1331–1386
39. Nagel K, Schreckenberg M (1992) A cellular automaton model for freeway traffic. *J Phys I* 2:2221–2229
40. Nakata M, Yamauchi A, Tanimoto J, Hagishima A (2010) Dilemma game structure hidden in traffic flow at a bottleneck due to a 2 into 1 lane junction. *Phys A* 389:5353–5361
41. Nowak M, May RM (1992) Evolutionary games and spatial chaos. *Nature* 359:826
42. Orosz G, Wilson RE, Stépán G (2010) Traffic jams: dynamics and control. *Phil Trans R Soc A* 368:4455–4479
43. Perc M (2007) Premature seizure of traffic flow due to the introduction of evolutionary games. *New J Phys* 9:3
44. Roughgarden T (2003) The price of anarchy is independent of the network topology. *J Comput Syst Sci* 67:341–364
45. Sugden R (1986) *The economics of rights, cooperation and welfare*. Blackwell, Oxford
46. Sun XY, Jiang R, Hao QY, Wang BH (2010) Phase transition in random walks coupled with evolutionary game. *Europhys Lett* 92:18003
47. Szabó G, Töke C (1998) Evolutionary prisoner’s dilemma game on a square lattice. *Phys Rev E* 58:69–73
48. Szilagyí MN (2006) Agent-based simulation of the n-person chicken game. In: Jorgensen S, Quincampoix M, Vincent TL (eds) *Advances in dynamical games*, vol 9. *Annals of the International Society of Dynamic Games*, Birkhäuser, Boston, pp 695–703
49. Tang TQ, Li CY, Huang HJ (2010) A new car-following model with the consideration of the driver’s forecast effect. *Phys Lett A* 374:3951–3956
50. Tanimoto J, Hagishima A, Tanaka Y (2010) Study of bottleneck effect at an emergency evacuation exit using cellular automata model, mean field approximation analysis, and game theory. *Phys A* 389:5611
51. von Neumann J, Morgenstern O (1944) *Theory of games and economic behaviour*. Princeton University Press, Princeton
52. Wahle J, Bazzan ALC, Klügl F, Schreckenberg M (2000) Decision dynamics in a traffic scenario. *Phys A* 287:669–681
53. Wahle J, Bazzan ALC, Klügl F, Schreckenberg M (2002) The impact of real-time information in a two-route scenario using agent-based simulation. *Transp Res Part C* 10:399–417
54. Wang WX, Wang BH, Zheng WC, Yin CY, Zhou T (2005) Advanced information feedback in intelligent transportation systems. *Phys Rev E* 72:066702
55. Wang WX, Ren J, Chen GR, Wang BH (2006) Memory-based snowdrift game on networks. *Phys Rev E* 74:056113

56. Wang XF, Zhuang J (2011) Balancing congestion and security in the presence of strategic applicants with private information. *Eur J Oper Res* 212:100–111
57. Xiang Z-T, Li Y-J, Chen Y-F, Xiong L (2013) Simulating synchronized traffic flow and wide moving jam based on the brake light rule. *Phys A* 392:5399–5413
58. Yamauchi A, Tanimoto J, Hagishima A, Sagara H (2009) Dilemma game structure observed in traffic flow at a 2-to-1 lane junction. *Phys Rev E* 79:036104
59. Zhao X-M, Xie D-F, Gao Z-Y, Gao L (2013) Equilibrium of a two-route system with delayed information feedback strategies. *Phys Lett A* 377:3161–3169
60. Zheng XP, Cheng Y (2011) Conflict game in evacuation process: a study combining cellular automata model. *Phys A* 390:1042